Asymptotic Homogenization for Modeling of Wingbox Structures

Demetra A. Hadjiloizi * and Paul M. Weaver †
Bernal Institute, University of Limerick, Ireland

The asymptotic homogenization technique has been used to analyze a wing box structure consisting of trapezoidally arranged reinforcements encased within thin rectangular plates. Ignoring stress concentration effects at the region of the overlap between the various components, the wingbox structure can be analyzed by handling each constituent independently from each other. To this end, a simpler structure was first considered which was made up of a base plate and a single stiffener web; the results were then extrapolated to those of the wingbox structure via superposition by adding in the contributions of each constituent of the overall unit cell. The work culminated in closed-form expressions for the effective in-plane elastic coefficients of the wingbox. This result demonstrates the attractiveness of the methodology in that it can be used in engineering analysis and design to customize the architecture of a thin-walled reinforced composite by changing some material or geometrical parameters of interest. Such parameters could be the material of the base plate, the spatial arrangement of the reinforcements, the relative sizes of the different constituents.

I. Introduction

Composite structures are predominantly used in the form of beams, plates and shells. Recent advancements in additive manufacturing and 4D printing [1, 2] facilitate the fabrication of these structures with wide-ranging architectures and geometries. Such progress renders plates and shells, including sandwich and reinforced structures, particularly attractive for many applications in lightweight construction, aerospace and automotive engineering, naval architecture and marine engineering, nanotechnology, biomedical engineering and sports equipment, e.g [3–6].

In the quest to solve structural problems through the use of judicially designed composite plates or shells, it would be advantageous if the macroscopic properties of these structures are known a priori. Then, a computationally simple model such as a beam embedded with effective properties represented by inherent complexity can be modeled. An effective way of achieving this objective is by means of appropriate mechanics-based models via which the macroscopic properties (elastic, thermal etc.) are correlated to the geometrical and material characteristics of the microstructure. In this context the term "macroscopic property" should be interpreted as a statistically averaged or global property of the structure at the continuum level. On the other hand, "microstructure" relates to the substructural spatial arrangement and characteristics of the constituents of the composite at the appropriate scale of inhomogeneity. The terms are not necessarily indicative of any actual length scale. In this paper for example, we are interested in determining the macroscopic properties of a wingbox structure in which the inhomogeneity or "microstructure" is generated by trapezoidally arranged stiffeners encased between thin horizontal rectangular plates and thin vertical spar webs.

It is imperative that these models are sufficiently comprehensive to capture the important underlying physics and, at the same time, be readily amenable to the analytical, semi-analytical or numerical analysis that is typically a prerequisite to engineering design; ideally these models culminate in closed-form design-oriented equations that can be incorporated into a simple spreadsheet program that permits the requisite iterations and modifications (with respect to the pertinent material and geometric parameters) in an expedient and efficient manner. Typically, hierarchical structures are characterized by a periodic or nearly periodic spatial configuration. As a consequence, their behavior involves the coupling of two vastly different scales; the microscopic or fast scale and the macroscopic or slow scale. The microscopic scale essentially zooms in on the periodicity or unit cell of the structure and describes the nature and spatial arrangement of the different constituents (reinforcements, matrix, sensors, actuators etc.). The macroscopic scale zooms out on the entire structure and is a manifestation of the global formulation of the problem as reflected by the external load distribution, support conditions etc. It is oblivious of what is going on inside the unit cell. Thus, it is apparent that micromechanical modeling of composites can best be implemented if the aforementioned two scales can

*Postdoctoral Researcher, University of Limerick and AIAA Member, email: demetra.hadjiloizi@ul.ie.
†Bernal Chair in Composite Materials and Structures, School of Engineering, and AIAA Member, email: Paul.Weaver@ul.ie.

be decoupled and treated separately. This process is tantamount to first obtaining a set of acceptable volume-averaged material coefficients to replace their actual rapidly-varying (a direct consequence of the microscopic scale) counterparts. These averaged coefficients, hereafter to be referred to as the effective coefficients, are then used in lieu of the actual coefficients in the macroscopic governing and constitutive equations to obtain displacements, strains, stresses and other desired field variables. One technique that can meet these objectives is that of asymptotic homogenization and the mathematical details can be found in [7–10]. Many problems of different length-scale in elasticity, thermoelasticity, piezoelasticity, fracture mechanics, design and optimization as they pertain to composite beams, plates and shells have been analyzed using asymptotic homogenization [11], [12] and can be found in the works of [12–20].

As previously mentioned, composite and reinforced thin walled structures in the form of beams, plates and shells have already been established as the prevalent structures in engineering and technology. Since most of these structures are periodic or nearly periodic the asymptotic homogenization method can be successfully employed to analyze both the macroscopic and local (microscopic) behavior. Our objective is to model an anisotropic thin-walled structure with material coefficients that are rapidly varying in magnitude (over the characteristic length scale of the structure) into a homogenized or "smeared" one characterized by the corresponding effective properties, see for example the works of [13, 14].

When discussing asymptotic homogenization modeling of thin-walled structures, it would be remiss to ignore the pioneering work of [21, 22]. In these works, Caillerie introduces two sets of microscopic variables; one set pertains to the tangential directions which are characterized by periodicity and the other variable relates to the transverse direction in which no periodicity exists. In [23, 24] the authors followed this approach in their study of the pure bending of a thin, linearly elastic homogeneous plate as did [25–30] in their investigation of composite and reinforced composite magnetoelectric plates. Examples of structures that have been analyzed are diagonally restrained reinforced plates, reinforced structures with a triangular arrangement of reinforcements, hexagonal honeycomb sandwich plates and rib-reinforced plates. Other relevant works can be found in [31–33].

The present paper deals with the elastic analysis of the wingbox configuration shown in Fig. 1 consisting of trapezoidally arranged stiffeners encased within thin rectangular plates. The general model developed by [27] constitutes the starting point of the present analysis; the geometrical parameters characterizing the structure under investigation are derived, the appropriate unit cell problems are identified and, finally, the effective elastic coefficients are determined. The work is implemented in steps; first a simpler structure consisting of a base plate and a single oriented stiffener web is analyzed. Once this basic unit is considered, the effective coefficients of the more general structure are obtained via superposition. In doing do, one accepts the error incurred at the regions of overlap of the various constituents because these regions are highly localized and do not contribute significantly to the integral over the volume of the unit cell, see [8], for a formal justification.

Following this introduction, the rest of the paper is organized as follows: The general problem formulation is presented in Section II and geometric set up is given in Section III . In addition, in Section IV the overall solution methodology is proposed. Section V applies the model to the wing box structure. Finally, Section VI concludes this work.

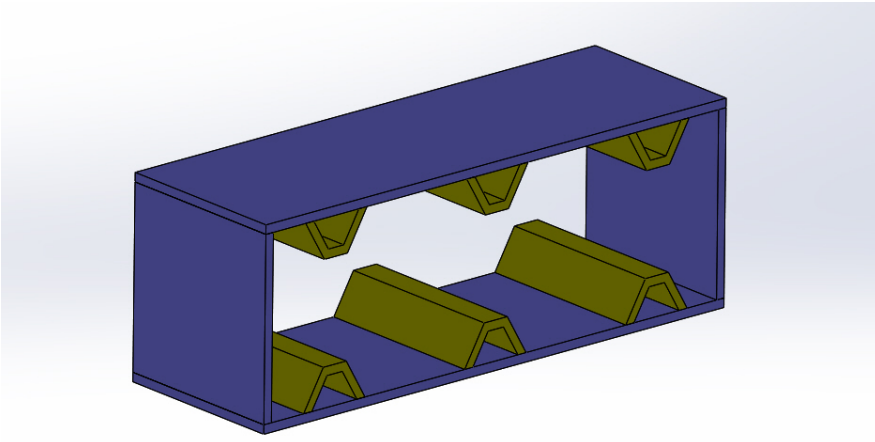

Fig. 1 Unit cell of Wingbox Structure with trapezoidal reinforcements.

II. General Problem Formulation

Consider a thin composite layer representing an inhomogeneous solid with rapidly varying thickness which is obtained by repeating a certain small unit cell Ω_t in the $x_1 - x_2$ plane Fig. 2. All three pertinent coordinates are assumed to have been made dimensionless by dividing by a certain characteristic dimension of the body, L. Note that the shape of the top surface of the plate is determined by the type of the surface reinforcement, for example the shape of stiffeners such as ribs, spars, stringers. In the particular case that no surface reinforcements are used this surface is plane.

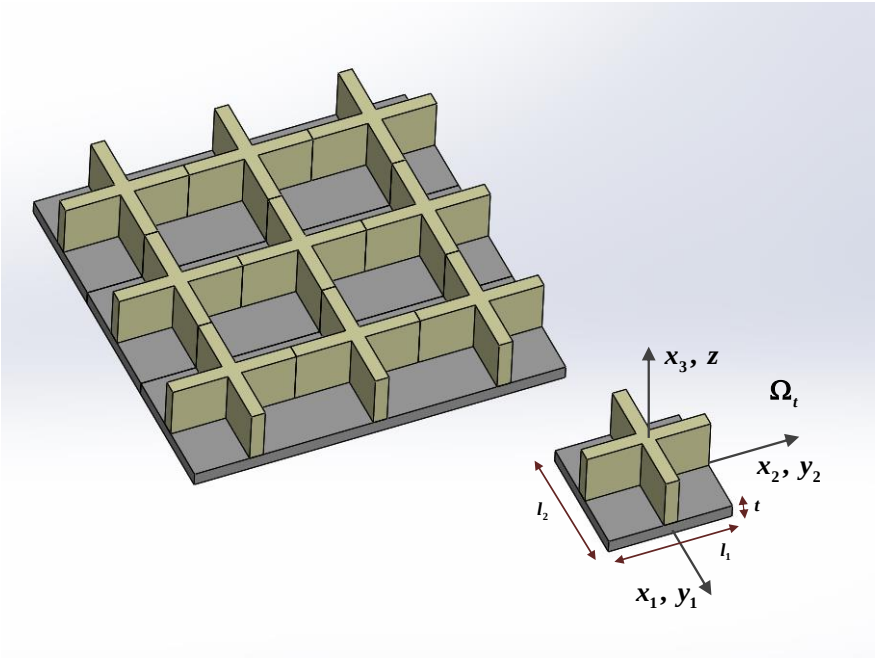

Fig. 2 Thin composite reinforced plate and its periodicity cell.

The shape of the layer and the structure of the material are assumed to be periodic in the coordinates x_1 and x_2, with the unit cell defined by the following inequalities:

$$\left\{ \frac{-l_1}{2} < x_1 < \frac{l_1}{2},\ \frac{-l_2}{2} < x_2 < \frac{l_2}{2},\ S^- < z < S^+ \right\} \tag{1}$$

where

$$S^{\pm} = \pm\frac{t}{2} \pm tF^{\pm}\left(\frac{x_1}{l_1}, \frac{x_2}{l_2}\right) \tag{2}$$

and l_1 and l_2 define the lateral dimensions of the unit cell as the product of the dimensionless thickness of the plate times the dimensionless length of the plate in x_1 and x_2 respectively, S^+ describes the profile of the top surface and $F^{\pm}$ defines its geometrical characteristics. The dimensionless thickness of the plate is denoted by t.

The elastic deformation of this periodic structure of Fig. 2 is described by means of the following expressions:

$$\begin{aligned} \frac{\partial \sigma_{ij}\left(x_i, \frac{x_\alpha}{l_\alpha},\right)}{\partial x_j} &= P_i\left(x_i, \frac{x_\alpha}{l_\alpha},\right) \\ \sigma_{ij}\left(x_i, \frac{x_\alpha}{l_\alpha}\right) &= C_{ijkl}\left(\frac{x_\alpha}{l_\alpha}\right)\frac{\partial u_k\left(x_i, \frac{x_\alpha}{l_\alpha}\right)}{\partial x_l} \\ \epsilon_{ij} &= \frac{1}{2}\left(\frac{\partial u_i\left(x_i, \frac{x_\alpha}{l_\alpha}\right)}{\partial x_j} + \frac{\partial u_j\left(x_i, \frac{x_\alpha}{l_\alpha}\right)}{\partial x_i}\right) \end{aligned} \tag{3}$$

Here σ_{ij} is the mechanical stress, P_i is a generic body force, u_i is the mechanical displacement, ϵ_{ij} is the second order strain field and C_{ijkl} is the tensor of the elastic coefficients. The standard summation convention for repeated indices is assumed.The first expression represents the force balance equation, the second is the constitutive equation and the third relates the strains to the displacements. The problem is constructed by two scales; the microscopic or "fast" scale which characterize the periodicity in the tangential directions of the plate and,superimposed on it, the macroscopic or "slow" scale which is a manifestation the global formulation of the problem. Thus, in the parlance of asymptotic homogenization, the microscopic variables are introduced as follows:

$$\begin{aligned} y_1 = \frac{x_1}{l_1}, \quad y_2 = \frac{x_2}{l_2}, \quad z = \frac{z}{t} \\ \frac{\partial}{\partial x_\alpha} = \frac{\partial}{\partial x_\alpha} + \frac{1}{l_\alpha}\frac{\partial}{\partial y_\alpha}, \quad \frac{\partial}{\partial z} = \frac{1}{t}\frac{\partial}{\partial z} \end{aligned} \tag{4}$$

Accordingly, the stipulation of periodicity in the tangential directions dictates that the dependent field variables are functions of both the microscopic (dependence on $\frac{x_\alpha}{l_\alpha}$ and z) and macroscopic variables (dependence onx_i), see [10, 13], whereas the material coefficients are strictly periodic.

Assume also that the top and bottom surfaces of the composite are subjected to surface tractions p_i which are related to stresses by Cauchy boundary conditions:

$$\sigma_{ij} n_j = p_i \qquad \text{on} \quad S^{\pm} \tag{5}$$

The asymptotic homogenization model pertinent to the analysis of the structure of Fig. 2 can be found in [27, 28] and, as mentioned before, constitute the starting point of the current work. Here, only a brief outline is given. The methodology begins by defining the microscopic variables, expanding the dependent field variables into infinite series of powers of small geometrical parameter, and finally substituting the resulting expressions in Eq. (3). This procedure decouples the macroscopic problem from its local microscopic counterpart which is characterized by the unit cell problem. Two unit cell problems can be extracted, one pertaining to in-plane and the other to out-of-plane deformation. The former unit cell problem, from which the effective extensional elastic coefficients may be determined, is given in [25], see Appendix A and is:

$$\begin{aligned} \frac{1}{\bar{l}_\beta}\frac{b^{\mu\alpha}_{i\beta}}{\partial y_\beta} + \frac{b^{\mu\alpha}_{i3}}{\partial z} = 0, \quad \text{with} \\ \frac{1}{\bar{l}_\beta} b^{\mu\alpha}_{i\beta} n^{\pm}_\beta + b^{\mu\alpha}_{i3} n^{\pm}_3 = 0, \quad \text{on} \quad S^{\pm} \end{aligned} \tag{6}$$

where

$$b^{\mu\alpha}_{ij} = \left(C_{ijk\alpha}\frac{1}{\bar{l}_\alpha}\frac{\partial}{\partial y_\alpha} + C_{ijk3}\frac{\partial}{\partial z} \right) N^{\mu\alpha}_k + C_{ijk\alpha} \tag{7}$$

Here, $n_i\pm$ are the components of the unit vector normal to the top, $\bar{l_\beta}$ denotes the length of the plate divide by the thickness, S^+, and bottom, S^-, surfaces of the structure of Fig. 2. In the language of the classical plate theory, $b^{\mu\alpha}_{ij}$ coefficients correspond to the plane stress reduced stiffness coefficients, Q_{ij} , see for example [34]; they are related as below:

$$Q_{\alpha\beta} = b^{\beta\beta}_{\alpha\alpha}, \;\; Q_{\alpha 6} = b^{12}_{\alpha\alpha}, \;\; Q_{66} = b^{12}_{12} \tag{8}$$

Once the coefficient functions are determined they are averaged over the volume of the unit cell to yield the aforementioned effective coefficients, $< b^{\mu\alpha}_{ij} >$. These coefficients correspond to the extensional stiffness matrix A. In other words, [13],

$$A_{\alpha\beta} = t^{(p)} < b^{\beta\beta}_{\alpha\alpha} >, \;\; A_{\alpha 6} = t^{(p)} < b^{12}_{\alpha\alpha} >, \;\; A_{66} = t^{(p)} < b^{12}_{12} > \tag{9}$$

where $t^{(p)}$ is the physical thickness obtained by multiplying dimensionless thickness with the characteristic length of the body. In turn, the coefficient functions are used as input to the macroscopic problem to compute the various field variables. For example, the familiar stress resultants appearing prominently in the classical composite plate theory, see for example in [34], are expressed as:

$$N_{\alpha\beta} = t^{(p)} < b^{\mu\nu}_{\alpha\beta} > \epsilon_{\mu\nu} - (t^{(p)})^2 < z b^{\mu\nu}_{\alpha\beta} > u_{3,x_\mu x_\nu} \tag{10}$$

In passing, we note that in Equations Roman letters, $i, j, k, \ldots$ vary from 1 to 3, while their Greek counterparts, α, β, μ, $\nu, \ldots$ assume values of 1 or 2 only.

III. Geometrical set-up

Our objective in this Section is to develop an asymptotic homogenization model for the analysis of the wingbox structure of Fig. 1. All the constituents are taken to be generally orthotropic.

The geometrical nature of the structure prompts us to first analyze a simple unit cell made up of only a base plate and a stiffener web, see Fig. 3. Once this is implemented, the resulting expressions for the entire wingbox can be obtained by superposition. Furthermore, with reference to the unit cell of Fig. 3, we seek to further break it down into its two constituents, the base plate and the stiffener web, so that each one can be handled independently. That such a procedure can be undertaken analytically, without recourse to numerical algorithms, has been demonstrated for different structures of varying complexity in [25–30, 35]. Furthermore, it underlines the main advantage of the asymptotic homogenization method in that it allows the extraction of closed-form expressions for the effective coefficients that can be readily used in design and analysis of arbitrary reinforced thin-walled structures.

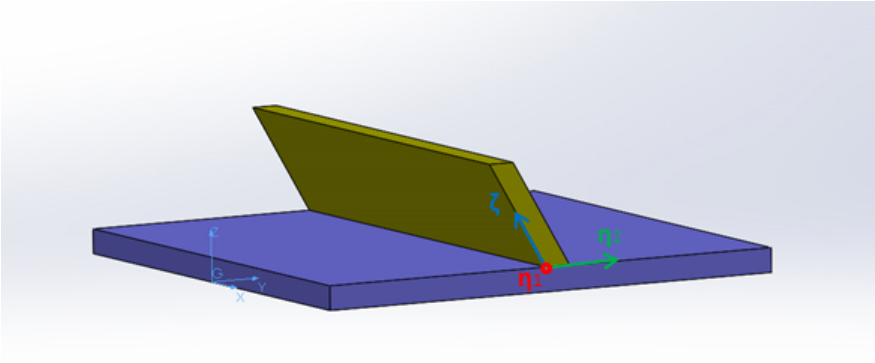

Fig. 3 Base plate and a stiffener web in $[y_1, y_2, z]$ and rotated $[\eta_1, \eta_2, \zeta]$ coordinate.

A quick glance at Fig. 1 reveals that the plane of the stiffener web (perpendicular to the thickness, t, dimension) of length L and height H is oriented at an angle φ with respect to the $x_1 - z$ plane. Thus, it becomes quite advantageous if we introduce another local coordinate system, $[\eta_1, \eta_2, \zeta]$, through rotation by an angle φ around the η_1. In this way, the stiffener is oriented entirely along the y_1 direction and the resulting differential equations depend only on η_2 and ζ. Having divested ourselves of one coordinate variable makes it easier to solve for the effective coefficients. Clearly, the two coordinate systems are related by,

$$\begin{aligned} \eta_2 &= y_2 \cos\varphi + z \sin\varphi \\ \zeta &= -y_2 \sin\varphi + z \cos\varphi \end{aligned} \tag{11}$$

and the derivatives transform according to:

$$\begin{aligned} \frac{\partial}{\partial y_2} &= \cos\varphi \frac{\partial}{\partial \eta_2} - \sin\varphi \frac{\partial}{\partial \zeta} \\ \frac{\partial}{\partial \zeta} &= \sin\varphi \frac{\partial}{\partial \eta_2} + \cos\varphi \frac{\partial}{\partial \zeta} \end{aligned} \tag{12}$$

Moving along, the unit vectors normal to the surfaces on which the boundary conditions must be supplied are readily determined as:

$$\begin{aligned} n_{\eta_2} &= \cos\varphi \eta_2 + \sin\varphi \zeta, \quad \text{on} \quad \eta_2 = \pm t/2 \\ n_\zeta &= -\sin\varphi \eta_2 + \cos\varphi \zeta, \quad \text{on} \quad \zeta = 1/2, 1/2 + H \end{aligned} \tag{13}$$

If we further assume that the $[\eta_1, \eta_2, \zeta]$ coordinate axes also coincide with the principal material axes of the orthotropic stiffener web (which is quite reasonable an assumption), then the elasticity tensor of this material with respect to the original $[x_1, x_2, x_3]$ or, equivalently, $[y_1, y_2, z]$ system is given as:

$$C_{ijkl} = \begin{bmatrix} C_{11} & C_{12} & C_{13} & C_{14} & 0 & 0 \\ C_{12} & C_{22} & C_{23} & C_{24} & 0 & 0 \\ C_{13} & C_{23} & C_{33} & C_{34} & 0 & 0 \\ C_{14} & C_{24} & C_{34} & C_{44} & 0 & 0 \\ 0 & 0 & 0 & 0 & C_{55} & C_{56} \\ 0 & 0 & 0 & 0 & C_{56} & C_{66} \end{bmatrix} \tag{14}$$

The relationship between the elastic coefficients appearing in Eq. (14) and the principal material coefficients is expressed via the familiar tensor transformation law for a 4th order tensor, namely

$$C_{ijkl} = a_{im} a_{jn} a_{kq} a_{lr} C^{(p)}_{mnqr} \tag{15}$$

where C_{ijkl} are the elastic properties referenced to the y_1, y_2, y_3 system and $C^{(p)}_{mnqr}$ are their principal material counterparts. Finally, a_{ij} are the direction cosines of the rotation defined by Eq. (11) i.e.,

$$a_{ij} = \begin{bmatrix} 1 & 0 & 0 \\ 0 & \cos\varphi & \sin\varphi \\ 0 & \sin\varphi & -\cos\varphi \end{bmatrix} \tag{16}$$

IV. Solution of the unit cell problem

In this section we provide the solution of the unit cell problem of the structure of Fig. 3. An important assumption of our model is that the structures under examination are piece-wise homogeneous. Consequently, in view of the coordinate transformation of Eq. (11), the unit cell problem of Eq. (6) is modified to:

$$\begin{aligned} &\frac{\partial}{\partial \eta_2}\left[\frac{\cos\varphi}{l_2} b^{\mu\alpha}_{i2} + \sin\varphi\, b^{\mu\alpha}_{i3}\right] + \frac{\partial}{\partial \zeta}\left[\frac{-\sin\varphi}{l_2} b^{\mu\alpha}_{i2} + \cos\varphi\, b^{\mu\alpha}_{i3}\right] = 0 \\ &\frac{\cos\varphi}{l_2} b^{\mu\alpha}_{i2} + \sin\varphi\, b^{\mu\alpha}_{i3} = \frac{-\cos\varphi}{l_2} C_{i2\mu\alpha} + \sin\varphi\, C_{i3\mu\alpha} \quad \text{on} \quad \eta_2 = \pm t/2 \\ &\frac{-\sin\varphi}{l_2} b^{\mu\alpha}_{i2} + \cos\varphi\, b^{\mu\alpha}_{i3} = \frac{\sin\varphi}{l_2} C_{i2\mu\alpha} - \cos\varphi\, C_{i3\mu\alpha} \quad \text{on} \quad \zeta = 1/2, 1/2 + H \end{aligned} \tag{17}$$

Let us begin by obtaining the approximate solution for the "22" type problem; which refers to the solution of the Eq. (17) for indices $\mu = 2,\ \alpha = 2$, and pertains to the in-plane elastic coefficients in y_2 direction; this follows directly from Eq. (17) and is readily determined to be:

$$\left.\begin{aligned} &\frac{\cos\varphi}{l_2} b^{\mu\alpha}_{i2} + \sin\varphi\, b^{\mu\alpha}_{i3} = \frac{-\cos\varphi}{l_2} C_{i2\mu\alpha} + \sin\varphi\, C_{i3\mu\alpha} \quad \text{on} \quad \eta_2 = \pm t/2 \\ &\frac{-\sin\varphi}{l_2} b^{\mu\alpha}_{i2} + \cos\varphi\, b^{\mu\alpha}_{i3} = \frac{\sin\varphi}{h_2} C_{i2\mu\alpha} + \cos\varphi\, C_{i3\mu\alpha} \quad \text{on} \quad \zeta = 1/2, 1/2 + H \end{aligned}\right\} \quad \text{Everywhere in the stiffener web} \tag{18}$$

From Eq. (7) and Eq. (18) we readily determine that:

$$\frac{\partial N^{22}_2}{\partial \eta_2} = -\frac{\cos\varphi}{l_2}, \quad \frac{\partial N^{22}_2}{\partial \zeta} = -\frac{\sin\varphi}{l_2}, \quad \frac{\partial N^{22}_3}{\partial \zeta} = \frac{\partial N^{22}_3}{\partial \eta_2} = 0 \tag{19}$$

Back-substituting into Eq. (7) reveals that the corresponding b^{22}_{ij} elastic coefficients vanish in the region of the stiffener web and we therefore conclude that only the base plate contributes to the in-plane stiffness in the y_2 direction, as will be determined shortly.

Reference to Fig. 1 reveals that the unit cell problem in the region of the base plate is best solved in the original $[y_2, y_2, z]$ coordinate system because periodicity considerations stipulate that the resulting differential equations are independent of y_1 and y_2 and only depend on z. One thus obtains the following expressions for the base plate:

$$\left.\begin{aligned} b_{11}^{22} = C_{21} - \frac{C_{13}C_{23}}{C_{33}} = Q_{12}^{(B)}, \quad b_{22}^{22(B)} = C_{22} - \frac{C_{23}^2}{C_{33}^2} = Q_{22}^{(B)} \\ b_{12}^{22} = b_{13}^{22} = b_{23}^{22} = b_{33}^{22} = 0 \end{aligned}\right\} \quad \text{In the region of the base plate} \tag{20}$$

The solution of the "12" problems proceeds in the same manner. In fact, in this case solution is quite trivial and is:

$$\begin{aligned} b_{11}^{12} = b_{22}^{12} = b_{12}^{12} = b_{13}^{12} = b_{33}^{12} = 0 \quad \text{In the region of the stiffener web} \\ b_{12}^{12} = C_{66} = Q_{66}^{(B)},\ b_{22}^{12} = 0,\ b_{11}^{12} = b_{12}^{13} = b_{12}^{23} = b_{33}^{12} = 0 \quad \text{In the region of the base} \end{aligned} \tag{21}$$

The solution of the "11" type problems proceeds in an identical manner and is:

$$\left.\begin{aligned} b_{11}^{11} = C_{11} + \frac{2C_{12}C_{13} - C_{12}^2C_{33} - C_{13}^2C_{22}}{C_{22}C_{33} - C_{23}^2} = Q_{11}^{(S)} \\ b_{11}^{22} = b_{12}^{11} = b_{23}^{11} = b_{13}^{11} = b_{33}^{11} = 0 \end{aligned}\right\} \quad \text{In the region of the stiffener web} \tag{22}$$

$$\left.\begin{aligned} b_{11}^{11} = C_{11} - \frac{C_{13}^2}{C_{33}} = Q_{11}^{(B)},\ b_{22}^{11} = C_{12} - \frac{C_{23}C_{13}}{C_{33}} = Q_{21}^{(B)} \\ b_{12}^{11} = b_{13}^{11} = b_{23}^{11} = b_{33}^{11} = 0 \end{aligned}\right\} \quad \text{In the region of the base plate} \tag{23}$$

We now proceed with the estimation of the in-plane effective coefficients which are obtained via integration of the pertinent coefficient functions in Eqs. (20)- (23) over the volume of the unit cell according to:

$$\langle \cdots \rangle = \int_\Omega (\cdots)\, dy_1 dy_2 dz \tag{24}$$

A straight forward application of Eq. (24) reveals the following expressions,

$$\begin{aligned} \langle 1 \rangle_S &= \int_\Omega d\eta_1 d\eta_2 d\zeta = \frac{Ht_2}{h_2} = F_S \\ \langle 1 \rangle_B &= \int_\Omega dy_1 dy_2 dz = 1 = F_B \end{aligned} \tag{25}$$

where the subscripts S and B denote the stiffener web and the base respectively and F_S is the cross-sectional area. The non-zero in-plane elastic coefficients are derived from Eqs. (20)- (23) as:

$$\begin{aligned} A_{11} &=< Q_{11} > = t^{(p)} \left(Q_{11}^{(B)} F_B + Q_{11}^{(S)} F_S \right) \\ A_{12} &=< Q_{12} > = t^{(p)} Q_{12}^{(B)} \\ A_{22} &=< Q_{22} > = t^{(p)} Q_{22}^{(B)} \\ A_{66} &=< Q_{66} > = t^{(p)} C_{66}^{(B)} \end{aligned} \tag{26}$$

where $< Q_{ij} >$ denotes the in-plane effective elastic coefficients.
Thus, the in-plane elastic coefficients for the geometrical set-up of Fig. 3 have been calculated. We will use the results to determine the corresponding effective coefficients of the wingbox structure.

V. Effective elastic coefficients for the wingbox structure

In this section we extrapolate the results obtained for the basic unit cell of Fig. 3 to their counterparts pertaining to the wingbox structure of Fig. 1. Due to symmetry of the structure we consider half of it as the unit cell. Consequently, the local problems can be solved in each region, where Ω_1 denotes the base plate, Ω_2 the stringer and Ω_3 the spar web, and by superposition the effective coefficients for the overall structure can be determined. As mentioned earlier on, the

contribution of each component of the wingbox is simply added without concern for the error incurred at the regions of overlap between these constituents. A complete mathematical justification for this argument in the form of the so-called principle of the split homogenized operator can be found in [8].

With reference to Fig. 4 which shows the requisite geometrical parameters and to the averaging procedure defined in Eq. (24), the final expressions for the effective in-plane elastic coefficients of the wingbox structure are given in Eq. (27). In arriving at these expressions, we shifted the $[\eta_1, \eta_2, \zeta]$ system from the middle of the lower base plate to the middle of the overall wingbox structure.

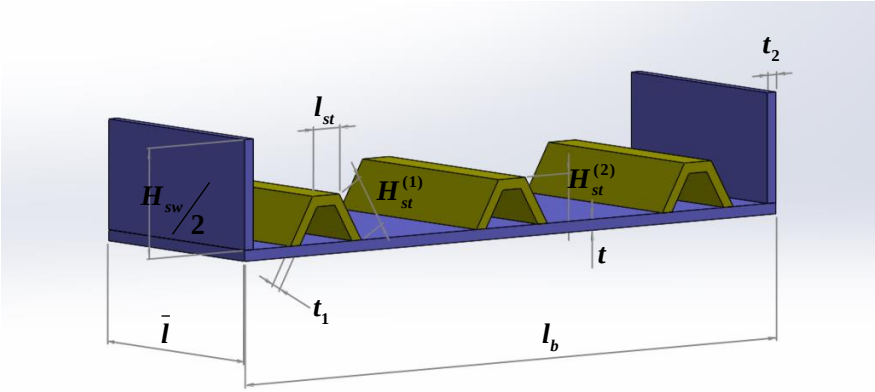

Fig. 4 Basic unit cell of the wingbox structure.

$$
\begin{aligned}
A_{11} &= 2t^{(p)}\left[\{Q_{11}\}^{(\bar{1})} + \{Q_{11}\}^{(\bar{2})}\left[\frac{6t_2H_{st}^1}{l_b} + \frac{3t_2l_{st}}{l_b}\right] + \{Q_{11}\}^{(\bar{3})}\frac{2t_2H_{sw}}{l_b}\right] \\
A_{12} &= 2t^{(p)}\left[\{Q_{12}\}^{(\bar{1})}\right] = A_{21}, \quad A_{22} = 2t^{(p)}\{Q_{22}\}^{(\bar{1})} \\
A_{66} &= 2t^{(p)}\{Q_{66}\}^{(\bar{1})}, \left\langle b_{12}^{11}\right\rangle = \left\langle b_{11}^{12}\right\rangle = \left\langle b_{12}^{22}\right\rangle = \left\langle b_{22}^{12}\right\rangle = \left\langle b_{i3}^{\nu\mu}\right\rangle = 0
\end{aligned}
\tag{27}
$$

In these expressions, each set of braces, $\{\dots\}$, is endowed with a superscript that reflects a particular region of the unit cell; region $(\bar{1})$ represents the base plate, region $(\bar{2})$ corresponds to the stringer and region $(\bar{3})$ pertains to the spar web. Consequently, the parameters within a set of braces, reflect the elastic coefficients of the material identified by the corresponding superscript.

We now turn to obtain the out-of plane effective elastic coefficients. Due to the symmetry of wingbox structure about the mid-plane, the effective coupling coefficients are zero. In other words,

$$
\langle B\rangle = (t^{(p)})^2\left\langle z b_{ij}^{mn}\right\rangle = 0 \tag{28}
$$

In order to determine the effective bending coefficients, we make use of the following expressions which are a consequence of Eq. (24):

$$
\begin{aligned}
\left\langle z^2\right\rangle_{\Omega_3} &= \frac{t_2}{12l_b}(H_{sw})^3 = I_{sw}, \;\; \left\langle z^2\right\rangle_{\Omega_1} = \frac{3H_{sw}^{(2)}t + 4t^3 + 6H_{sw}t^2}{12} = I_b \\
\left\langle z^2\right\rangle_{\Omega_{2,horizontal}} &= \frac{l_{st}t_1}{12l_b}\left[3(2H_{st}^{(2)} - H_{sw})(2H_{st}^{(2)} - H_{sw} - 2t_1^2) + 4t_1^3\right] = I_{st}^{(2)} \\
\left\langle z^2\right\rangle_{\Omega_{2,inclined}} &= \sin^2\varphi\frac{t_1^3H_{st}^{(1)}}{12l_b} + \frac{\cos\varphi H_{st}^{(1)}t_1}{12l_b}\Big[3(-H_{sw} + 2\cos\varphi H_{st}^{(2)})(-H_{sw} + 2\cos\varphi H_{st}^{(2)} - 2H_{st}^{(1)}) \\
&\quad + 4((H_{st}^{(1)})^2\cos\varphi)\Big] = I_{st}^{(1)}
\end{aligned}
\tag{29}
$$

Here I_i represent the second moments of area of the cross sections of the reinforcing elements Ω_i. With this regards, the non-vanish effective bending coefficients of the overall structure are obtained as follows:

$$
\begin{aligned}
D_{11} &= 2(t^{(p)})^3 \left[\{Q_{11}\}^{(\bar{1})} I_b + 3 \{Q_{11}\}^{(\bar{2})} (I_{st}^{(2)} + 2I_{st}^{(1)}) + \{Q_{11}\}^{(\bar{3})} I_{sw} \right] \\
D_{12} &= 2(t^{(p)})^3 \{Q_{12}\}^{(\bar{1})} I_b = D_{21}, \quad D_{22} = 2(t^{(p)})^3 \{\bar{Q}_{22}\}^{(\bar{1})} I_b
\end{aligned} \tag{30}
$$

The effective torsional stiffness coefficient,D_{66} can not be obtained in a closed form expression by means of the mechanics model used in this paper. Thus, we are forced to seek an approximate solution on the basis of the theory of torsion of thin-walled closed beams section [36]. We assume that the shear flow in the outer box is q_1 and the corresponding flows in each cell are $q_2 - q_7$ respectively, see Fig. 5 The angle of twist for the outer skin is readily

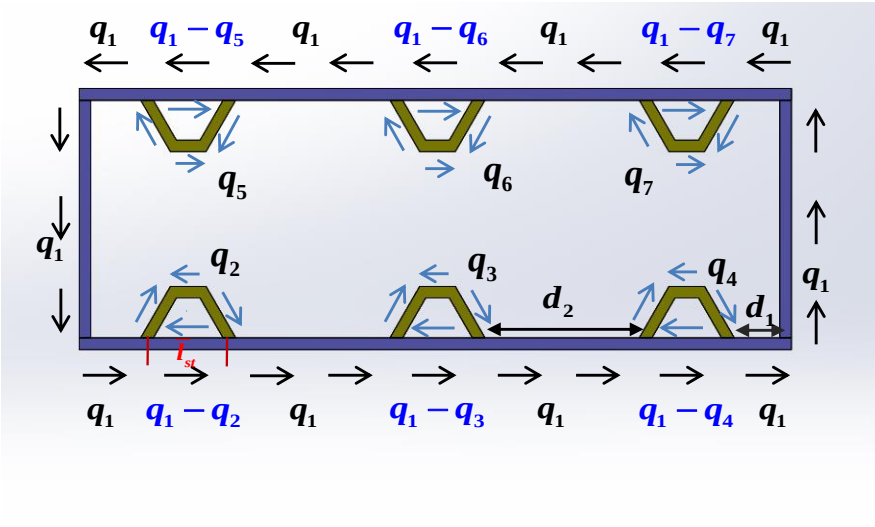

Fig. 5 Torsional shear flow.

computed as,

$$
\theta_1 = \frac{a_{66}}{2A_1} \left[\frac{4q_1 d_1}{t} + \frac{4q_1 d_2}{t} + \frac{4q_1 H_{sw}}{t_2} + \frac{\bar{l}_{st}}{t_1} \left[6q_1 - \sum_{n=2}^{7} q_i \right] \right] \tag{31}
$$

where A_1 is the enclosed area of the outer skin, d_1 is the distance between the stringer and the spar web and d_2 is the distance between the stringers and a_{66} is the element of the compliance matrix A . The angle of twist of i^{th} cell is given below:

$$
\theta_i = \frac{a_{66}}{2A_i} \left[\left[\frac{2H_{st}^1 + \bar{l}_{st}}{t_1} \right] q_i - \frac{q_1 - q_i}{t} \bar{l}_{st} \right] \tag{32}
$$

We also assume that the angle of twist is the same for all cells, i.e

$$
\theta_1 = \theta_2 = \theta_3 = \ldots \theta_7 = \theta \tag{33}
$$

Then, equations (31) and (32) constitute a linear system of seven unknows q_i, $i = 1, ..7$, from the solutions of which each shear flow can be determined in terms of the angle of twist θ, see Appendix B. As well, the torsional moment is given by,

$$
T = 2A_1 q_1 + 2 \sum_{i=2}^{7} A_i q_i \tag{34}
$$

Substituting the expressions of the shear flows into (34) and dividing by θ gives the approximate solution fo the torsional stiffness for the wingbox structure. The rather lengthy expression is given in Appendix B.

VI. Conclusion

The asymptotic homogenization technique was used to analyze a wingbox structure made up of reinforcing elements arranged in a trapezoidal configuration. The premise of asymptotic homogenization is that it successfully decouples the

microscopic or local problem which is a function of the substructural variations within the periodicity cell, namely the number, properties and spatial orientation of the reinforcing elements, from the macroscopic problem which is a manifestation of the global formulation. The local problem yields the so-called unit cell problems from which the effective in-plane elastic coefficients are extracted. In the case of the wingbox, the requisite unit cell problem with associated boundary conditions was solved in each region of the unit cell and then the results were superposed to obtain the effective elastic coefficients of the entire structure. In adhering to this methodology, we are ignoring complications arising at regions of overlap or intersection of the various constituents of the unit cell; these regions are highly localized and do not contribute significantly to the integral over the volume of the unit cell. The methodology followed in this work culminated in closed-form expressions for the elastic coefficients; this shows the usefulness of asymptotic homogenization models in engineering analysis and design since they can be applied to arbitrary thin-walled structures with different architectures.

Appendix A

In this Appendix a brief overview of work presented in [27] is given. Only the salient features are shown here. In particular, details of the development of the unit cell problem pertinent to the homogenized model in (6) is given.

The process begins with the introduction of the "fast" variables as defined by (4). The next step pertains to the expansion of the dependent field variables in powers of t as follows:

$$\begin{aligned} u_i(\mathbf{x},\mathbf{y},z) &= u_i^{(0)}(\mathbf{x}) + t u_i^{(1)}(\mathbf{x},\mathbf{y},z) + t^2 u_i^{(2)}(\mathbf{x},\mathbf{y},z) + O(t^3) \\ \sigma_{ij}(\mathbf{x},\mathbf{y},z) &= \sigma_{ij}^{(0)}(\mathbf{x},\mathbf{y},z) + t\sigma_{ij}^{(1)}(\mathbf{x},\mathbf{y},z) + t^2\sigma_{ij}^{(2)}(\mathbf{x},\mathbf{y},z) + O(t^3) \end{aligned} \tag{A.1}$$

Substituting (A.1) into the equilibrium equation in (3) and comparing terms with like powers of t results in the following expressions:

$$\begin{aligned} \frac{1}{\bar{l}_a}\sigma_{i\alpha,\alpha y}^{(0)} + \sigma_{i3,z}^{(0)} &= 0 \\ \sigma_{i\alpha,\alpha x}^{(0)} + \frac{1}{\bar{l}_a}\sigma_{i\alpha,\alpha y}^{(0)} + \sigma_{i3,z}^{(1)} &= 0 \\ \sigma_{i\alpha,\alpha x}^{(1)} + \frac{1}{\bar{l}_a}\sigma_{i\alpha,\alpha y}^{(2)} + \sigma_{i3,z}^{(2)} &= f_i \\ \sigma_{i\alpha,\alpha x}^{(2)} + \frac{1}{\bar{l}_a}\sigma_{i\alpha,\alpha y}^{(3)} + \sigma_{i3,z}^{(3)} &= g_i \\ \sigma_{i\alpha,\alpha x}^{(n)} + \frac{1}{\bar{l}_a}\sigma_{i\alpha,\alpha y}^{(n+1)} + \sigma_{i3,z}^{(n+1)} &= 0,\ n \geq 0 \end{aligned} \tag{A.2}$$

where

$$\begin{aligned} \sigma_{ij}^{(0)} &= c_{ijk\alpha}[u_{k,ax}^{(0)} + \bar{l}_\alpha^{-1}u_{k,ay}^{(1)} + c_{ilk3}u_{k,z}^{(1)}] \\ \sigma_{ij}^{(n)} &= c_{ijk\alpha}[u_{k,ax}^{(n)} + \bar{l}_\alpha^{-1}u_{k,ay}^{(n+1)} + c_{ilk3}u_{k,z}^{(n+1)}],\ n \geq 1 \end{aligned} \tag{A.3}$$

Here $\bar{l}_\alpha$ is the ratio of the dimensionless length (in direction x_i) to the dimensionless thickness of the plate. In other words,

$$\bar{l}_\alpha = \frac{l_\alpha}{t} \tag{A.4}$$

For the sake of economy of notation in (A.2) in the sequel we adopt the following short hand convention:

$$\frac{\partial \sigma_{ij}}{\partial x_j} = \sigma_{ij,jx} \tag{A.5}$$

Averaging (A.2) in the sense of (24) and using, at the same time, the boundary conditions in (5) we obtain the

following expressions for the stress and moment resultants,

$$\begin{aligned} &N^{(0)}_{\alpha\beta,x\beta} = 0,\ N^{(1)}_{\alpha\beta,x\beta} + tr^*_a(x_\gamma) = t\langle f_a\rangle, \\ &N^{(n)}_{\alpha\beta,x\beta} = 0 \quad \text{where} \quad n \geq 2 \\ &Q^{(1)}_{\beta,x\beta} = 0, \quad Q^{(2)}_{\beta,x\beta} + tq^*_3(x_\gamma) = t\langle g_3\rangle, \\ &Q^{(n)}_{\beta,x\beta} = 0 \quad \text{where} \quad n \geq 3 \end{aligned} \tag{A.6}$$

and

$$\begin{aligned} &M^{(0)}_{\alpha\beta,x\beta} + t\langle Q^{(1)}_a\rangle = 0, \\ &M^{(1)}_{\alpha\beta,x\beta} + t^2\rho^*_a(\mathbf{x}) - t\langle Q^{(2)}_a\rangle = t^2\langle z f_a\rangle \\ &M^{(2)}_{\alpha\beta,x\beta} - t\langle Q^{(3)}_a\rangle = 0, \\ &\langle z\sigma^{(2)}_{3\beta,x\beta} + \sigma^*_3(\mathbf{x}) = \langle z g_3\rangle \\ &M^{(n)}_{\alpha\beta,x\beta} = 0 \quad \text{where} \quad n \geq 3 \end{aligned} \tag{A.7}$$

where we define:

$$\begin{aligned} r^*_a(\mathbf{x}) &= \int_{-1/2}^{1/2}\int_{-1/2}^{1/2} (\omega^+ r^+_a + \omega^- r^-_a) dy_1 dy_2 \\ q^*_3(\mathbf{x}) &= \int_{-1/2}^{1/2}\int_{-1/2}^{1/2} (\omega^+ q^+_3 + \omega^- q^-_3) dy_1 dy_2 \end{aligned} \tag{A.8}$$

$$\begin{aligned} \rho^*_a(\mathbf{x}) &= \int_{-1/2}^{1/2}\int_{-1/2}^{1/2} (z^+\omega^+ r^+_a + z^-\omega^- r^-_a) dy_1 dy_2 \\ \sigma^*_3(\mathbf{x}) &= \int_{-1/2}^{1/2}\int_{-1/2}^{1/2} (z^+\omega^+ q^+_3 + z^-\omega^- q^-_3) dy_1 dy_2 \end{aligned} \tag{A.9}$$

We now proceed to the determination of the leading terms in the asymptotic expansion of the mechanical displacement. To this end, substitution of the first term of the (A.1),defined in (A.3) for $n = 0$ into the first and second expressions ($n = 1$) of (A.2), keeping at the same time, the boundary conditions in mind (5), results in the following boundary value problem:

$$\begin{aligned} D_{ik}u^{(1)}_k &= -C_{ik\alpha}(\mathbf{y}, z)u(\mathbf{x})^{(0)}_{k,\alpha x} \\ [L_{ijk}u^{(1)}_k + c_{ijk\alpha}u_{k,\alpha x}]N^\pm_j,\ &on\ Z^\pm \end{aligned} \tag{A.10}$$

Here, the differential operators are defined as below,

$$\begin{aligned} L_{ijk} &= c_{ijk\alpha}\frac{1}{\bar{l}_\alpha}\frac{\partial}{\partial y_\alpha} + c_{ijk3}\frac{\partial}{\partial z} \\ D_{ij} &= \frac{1}{\bar{l}_\alpha}\frac{\partial}{\partial y_\alpha}L_{i\alpha j} + \frac{\partial}{\partial z}L_{i3j} \end{aligned} \tag{A.11}$$

and the parameter $C_{ik\alpha}$ as,

$$C_{ik\alpha} = \frac{1}{\bar{l}_\alpha}\frac{\partial c_{i\beta k\alpha}}{\partial y_\beta} + \frac{\partial c_{i3k\alpha}}{\partial z} \tag{A.12}$$

The separation of variables on the right hand side of the (A.10) equation prompts us to assume the following form for the solution of $\mathbf{u}^{(1)}$,

$$u^{(1)}_i(\mathbf{x}, \mathbf{y}, z) = N^{k\alpha}_i(\mathbf{y}, z)\frac{\partial u^{(0)}_k}{\partial x_\alpha} + \omega_i(x) \tag{A.13}$$

where $N^{k\alpha}_i$ are the so called "local functions". Back substitution of (A.13) into the (A.10) results in the following unit cell problem,

$$\begin{aligned} &\frac{1}{\bar{l}_\beta}\frac{b_{i\beta}^{\mu\alpha}}{\partial y_\alpha} + \frac{b_{i3}^{\mu\alpha}}{\partial z} = 0, \quad \text{with} \\ &\frac{1}{\bar{l}_\beta} b_{i\beta}^{\mu\alpha} n_\beta^\pm + b_{i3}^{\mu\alpha} n_3^\pm = 0, \quad \text{on} \quad S^\pm \end{aligned} \tag{A.14}$$

where

$$b_{ij}^{\mu\alpha} = L_{ijk} N_k^{\mu\alpha} + C_{ijk\alpha} \tag{A.15}$$

In the analysis of the homogenized plate model the possibility of finding an exact solution often plays a significant role. In our case an exact solution for $k, \alpha = 1, 3$ and $3, 2$ can be readily found from (A.14) and is

$$\begin{aligned} N_1^{31} = -z; \;\; N_2^{31} = 0; \;\; N_1^{32} = 0 \\ N_2^{32} = -z; \;\; N_2^{31} = 0; \;\; N_3^{32} = 0 \end{aligned} \tag{A.16}$$

Thus, it follows that

$$b_{ij}^{31} = b_{ij}^{32} = 0 \tag{A.17}$$

With these solutions, expressions (A.13) can be simplified as follows:

$$\begin{aligned} u_1^{(1)} &= -z u_{3,1x}^{(0)} + N_1^{\beta\alpha} u_{\beta,\alpha x}^{(0)} + \omega_1(x) \\ u_2^{(1)} &= -z u_{3,2x}^{(0)} + N_2^{\beta\alpha} u_{\beta,\alpha x}^{(0)} + \omega_2(x) \\ u_3^{(1)} &= N_3^{\beta\alpha} u_{\beta,\alpha x}^{(0)} + \omega_3(x) \end{aligned} \tag{A.18}$$

We now move on to the determination of the leading term in the asymptotic expansion for mechanical stress. Substitution of (A.13) into the first expression of (A.3) and averaging leads to the following expression:

$$< \sigma_{ij}^{(0)} > = < b_{ij}^{\alpha\beta} > u_{\alpha,\beta x}^{(0)} \tag{A.19}$$

Subsequently, substitution of (A.19) into the first expression of (A.6) reveals, in comjuction with the boundary conditions, that

$$u_\alpha^{(0)} = 0 \quad \text{and} \quad \sigma_{ij}^{(0)} = 0 \tag{A.20}$$

To this end, the expressions in (A.18) may be written down as follows:

$$\begin{aligned} u_1^{(1)} &= -z u_{3,1x}^{(0)} \omega_1(x) \\ u_2^{(1)} &= -z u_{3,2x}^{(0)} + \omega_2(x) \\ u_3^{(1)} &= \omega_3(x) \end{aligned} \tag{A.21}$$

We now proceed to obtain the next term, $\sigma_{ij}^{(1)}$, of the mechanical stress field expansion. As such, we substitute expressions (A.21) into the second expression in (A.3) and to arrive at the following equation:

$$\sigma_{ij}^{(1)} = c_{ij\alpha\beta}\left[-z u_{3,\alpha\beta x}^{(0)} + \omega_{\alpha,\beta x}\right] + c_{ij3\beta}\omega_{3,\beta x} + c_{ijk\beta}\bar{l}_\beta^{-1} u_{k,\beta y}^{(2)} + c_{ijk3} u_{k,z}^{(2)} \tag{A.22}$$

Combination of this equation with (A.2) leads to the following system:

$$\begin{aligned} D_{ik} u_k^{(2)} &= (c_{i3b\beta\alpha} + z C_{i\alpha\beta} u_{3,x_a x_\beta}^{(0)}) \\ [L_{ijk} u_k^{(2)} &- z c_{ij\alpha\beta} u_{3,x_\alpha x_\beta}^{(0)}] N_j^\pm, \; on \; Z^\pm \end{aligned} \tag{A.23}$$

As previously, the solution of (A.23) may be written down as:

$$u_i^{(2)} = -N_i^{(1)\alpha\beta} u_{3,x_\alpha x_\beta}^{(0)} + \omega_i^{(*)}(x) \tag{A.24}$$

Following the same procedure as before we arrive at the second unit cell problem,

$$\begin{aligned} &\frac{1}{\bar{l}_\beta}\frac{b_{i\beta}^{(1)\mu\alpha}}{\partial y_\beta} + \frac{b_{i3}^{(1)\mu\alpha}}{\partial z} = 0, \quad \text{with} \\ &\frac{1}{\bar{l}_\beta} b_{i\beta}^{(1)\mu\alpha} n_\beta^{\pm} + b_{i3}^{(1)\mu\alpha} n_3^{\pm} = 0, \quad \text{on} \quad S^{\pm} \end{aligned} \tag{A.25}$$

where

$$b_{ij}^{(1)\mu\alpha} = L_{ijk} N_k^{(1)\mu\alpha} + z C_{ijk\alpha} \tag{A.26}$$

The presence of z coordinate in (A.26) reveals that the unit cell problem (A.25) is related to out-of-plane deformation of the homogenized reinforced plate.

Finally, using the results of this Appendix allow us to write down the stress and moment resultants pertaining to the homogenized plate in a form familiar to the classical composite laminate theory, see for example [34]. Thus:

$$\begin{aligned} N_{\alpha\beta} &= t < b_{\alpha\beta}^{\mu\nu} > \epsilon_{\mu\nu} - t^2 < b_{\alpha\beta}^{(1)\mu\nu} > u_{3,x_\mu x_\nu} \\ M_{\alpha\beta} &= t^2 < z b_{\alpha\beta}^{\mu\nu} > \epsilon_{\mu\nu} - t^3 < z b_{\alpha\beta}^{(1)\mu\nu} > u_{3,x_\mu x_\nu} \end{aligned} \tag{A.27}$$

Appendix B

The solution of the system (31) and (32) in terms of θ is shown below:

$$\begin{aligned} q_1 &= \theta \frac{3\delta_{12} + 3\delta_{13} - \delta_{22}}{3\delta_{12}\delta_{21} - \delta_{11}\delta_{22} + 3\delta_{13}\delta_{21}} = \theta \frac{\Delta_1}{\Delta_8} \\ q_2 = q_3 = \ldots = q_7 &= \theta \frac{\delta_{21} - \delta_{11}}{3\delta_{12}\delta_{21} - \delta_{11}\delta_{22} + 3\delta_{13}\delta_{21}} = \frac{\Delta_2}{\Delta_8}, \; i = 2, ..7 \end{aligned} \tag{B.1}$$

where,

$$\begin{aligned} \delta_{11} &= \frac{a_{66}}{2A_1}\left(\frac{4d_1}{t} + \frac{4d_2}{t} + \frac{4H_{sw}}{t_2} + \frac{6\bar{l}_{st}}{t_1}\right) \\ \delta_{12} &= -\frac{a_{66}\bar{l}_{st}}{2A_2 t}, \; \delta_{13} = -\frac{a_{66}\bar{l}_{st}}{2A_1 t} \\ \delta_{22} &= \frac{a_{66}}{2A_2}\left(\frac{2H_{st}^1}{t_1} + \frac{l_{st}}{t_1} + \frac{\bar{l}_{st}}{t}\right) \end{aligned} \tag{B.2}$$

Substituting (B.1) into (34) results in the following expression:

$$\theta = \frac{T\Delta_8}{2A_1\Delta_1 + 12A_2\Delta_2} = \frac{T\Delta_8}{\Delta_9} \tag{B.3}$$

Therefore, the torsional stiffness coefficient is given by:

$$\theta = a_{66}\frac{\Delta_9}{\Delta_8} \tag{B.4}$$

Acknowledgments

The authors would like to thank Science Foundation Ireland (SFI) for funding Spatially and Temporally VARIable COMPsite Structures (VARICOMP) Grant No. (15/RP/2773) under its Research Professor programme.

References

[1] Compton, B. G., and Lewis, J. A., "3D-printing of lightweight cellular composites," *Advanced materials*, Vol. 26, No. 34, 2014, pp. 5930–5935.

[2] Campbell, I., Bourell, D., and Gibson, I., "Additive manufacturing: rapid prototyping comes of age," *Rapid prototyping journal*, Vol. 18, No. 4, 2012, pp. 255–258.

[3] Mouritz, A., Gellert, E., Burchill, P., and Challis, K., "Review of advanced composite structures for naval ships and submarines," *Composite structures*, Vol. 53, No. 1, 2001, pp. 21–42.

[4] Lachenal, X., Daynes, S., and Weaver, P. M., "Review of morphing concepts and materials for wind turbine blade applications," *Wind Energy*, Vol. 16, No. 2, 2013, pp. 283–307.

[5] Daynes, S., and Weaver, P. M., "Review of shape-morphing automobile structures: concepts and outlook," *Proceedings of the Institution of Mechanical Engineers, Part D: Journal of Automobile Engineering*, Vol. 227, No. 11, 2013, pp. 1603–1622.

[6] Thill, C., Etches, J., Bond, I., Potter, K., and Weaver, P., "Composite corrugated structures for morphing wing skin applications," *Smart Materials and Structures*, Vol. 19, No. 12, 2010, p. 124009.

[7] Bensoussan, A., Lions, J.-L., and Papanicolaou, G., *Asymptotic analysis for periodic structures*, Vol. 5, North-Holland Publishing Company Amsterdam, 1978.

[8] Bakhvalov, N. S., and Panasenko, G., *Homogenisation: averaging processes in periodic media: mathematical problems in the mechanics of composite materials*, Vol. 36, Springer Science & Business Media, 2012.

[9] Sanchez-Palencia, E., "Homogenization of second order equations," *Non-Homogeneous Media and Vibration Theory*, 1980, pp. 45–83.

[10] Cioranescu, D., and Donato, P., "An introduction to homogenization, volume 17 of Oxford Lecture Series in Mathematics and its Applications," *The Clarendon Press Oxford University Press, New York*, Vol. 4, 1999, p. 118.

[11] Hadjiloizi, D., Georgiades, A., Kalamkarov, A., and Jothi, S., "Micromechanical modeling of piezo-magneto-thermo-elastic composite structures: Part I–Theory," *European Journal of Mechanics-A/Solids*, Vol. 39, 2013, pp. 298–312.

[12] Hadjiloizi, D., Georgiades, A., Kalamkarov, A., and Jothi, S., "Micromechanical modeling of piezo-magneto-thermo-elastic composite structures: Part II–Applications," *European Journal of Mechanics-A/Solids*, Vol. 39, 2013, pp. 313–327.

[13] Kalamkarov, A. L., "Composite and Reinforced Elements of Constructions," *John Wiley & Sons Ltd, Baffins Lane, Chichester, West Sussex PO 19 1 UD, UK, 1992. 286*, 1992.

[14] Kalamkarov, A. L., and Kolpakov, A. G., *Analysis, design, and optimization of composite structures*, Wiley, 1997.

[15] Devries, F., Dumontet, H., Duvaut, G., and Léné, F., "Homogenization and damage for composite structures," *International Journal for Numerical Methods in Engineering*, Vol. 27, No. 2, 1989, pp. 285–298.

[16] Guedes, J., and Kikuchi, N., "Preprocessing and postprocessing for materials based on the homogenization method with adaptive finite element methods," *Computer methods in applied mechanics and engineering*, Vol. 83, No. 2, 1990, pp. 143–198.

[17] Dasgupta, A., and Agarwal, R. K., "Orthotropic thermal conductivity of plain-weave fabric composites using a homogenization technique," *Journal of Composite Materials*, Vol. 26, No. 18, 1992, pp. 2736–2758.

[18] Yi, Y.-M., Park, S.-H., and Youn, S.-K., "Asymptotic homogenization of viscoelastic composites with periodic microstructures," *International Journal of Solids and Structures*, Vol. 35, No. 17, 1998, pp. 2039–2055.

[19] Aboudi, J., "Micromechanical analysis of fully coupled electro-magneto-thermo-elastic multiphase composites," *Smart materials and structures*, Vol. 10, No. 5, 2001, p. 867.

[20] Hassan, E., Georgiades, A., Savi, M., and Kalamkarov, A., "Analytical and numerical analysis of 3D grid-reinforced orthotropic composite structures," *International Journal of Engineering Science*, Vol. 49, No. 7, 2011, pp. 589–605.

[21] Caillerie, D., "Equations de la diffusion stationnaire dans un domaine comportant une distribution périodique d'inclusions aplaties de grande conductivité," *CR Acad. Sci., Ser. I: Math*, Vol. 292, No. 1, 1981, pp. 115–118.

[22] Caillerie, D., "Homogénéisation des équations de la diffusion stationnaire dans les domaines cylindriques aplatis," *RAIRO. Analyse numérique*, Vol. 15, No. 4, 1981, pp. 295–319.

[23] Kohn, R. V., and Vogelius, M., "A new model for thin plates with rapidly varying thickness," *International Journal of Solids and Structures*, Vol. 20, No. 4, 1984, pp. 333–350.

[24] Kohn, R. V., and Vogelius, M., "A new model for thin plates with rapidly varying thickness. III. Comparison of different scalings," *Quarterly of applied mathematics*, Vol. 44, No. 1, 1986, pp. 35–48.

[25] Hadjiloizi, D., Kalamkarov, A., and Georgiades, A., "Plane stress analysis of magnetoelectric composite and reinforced plates: Micromechanical modeling and application to laminated structures," *ZAMM-Journal of Applied Mathematics and Mechanics/Zeitschrift für Angewandte Mathematik und Mechanik*, 2017.

[26] Hadjiloizi, D., Kalamkarov, A., and Georgiades, A., "Plane stress analysis of magnetoelectric composite and reinforced plates: Applications to wafer-and rib-reinforced plates and three-layered honeycomb shells," *ZAMM-Journal of Applied Mathematics and Mechanics/Zeitschrift für Angewandte Mathematik und Mechanik*, 2017.

[27] Hadjiloizi, D., Kalamkarov, A., Metti, C., and Georgiades, A., "Analysis of Smart Piezo-Magneto-Thermo-Elastic Composite and Reinforced Plates: Part I–Model Development," 2014.

[28] Hadjiloizi, D., Kalamkarov, A., Metti, C., and Georgiades, A., "Analysis of Smart Piezo-Magneto-Thermo-Elastic Composite and Reinforced Plates: Part II–Applications," *Curved and Layered Structures*, Vol. 1, No. 1, 2014.

[29] Hadjiloizi, D., Kalamkarov, A., Saha, G., Christoforidis, K., and Georgiades, A., "Micromechanical modeling of thin composite and reinforced magnetoelectric plates–Effective elastic, piezoelectric and piezomagnetic coefficients," *Composite Structures*, Vol. 172, 2017, pp. 102–118.

[30] Hadjiloizi, D., Kalamkarov, A., Saha, G., Christofi, I., and Georgiades, A., "Micromechanical modeling of thin composite and reinforced magnetoelectric plates–Effective electrical, magnetic, thermal and product properties," *Composites Part B: Engineering*, Vol. 113, 2017, pp. 243–269.

[31] Duvaut, G., and Metellus, A., "Homogénéisation d'une plaque mince en flexion de structure périodique et symétrique," *Comptes Rendus de l'Académie des Sciences, Paris*, Vol. 283, 1976, pp. 947–950.

[32] Andrianov, I., Lesnichaya, V., and Manevich, L., "Homogenization methods in the statics and dynamics of ribbed shells," , 1985.

[33] Bravo-Castillero, J., Rodríguez-Ramos, R., Mechkour, H., Otero, J. A., and Sabina, F. J., "Homogenization of magneto-electro-elastic multilaminated materials," *The Quarterly Journal of Mechanics & Applied Mathematics*, Vol. 61, No. 3, 2008, pp. 311–332.

[34] Gibson, R. F., *Principles of composite material mechanics*, CRC press, 2016.

[35] Hadjiloizi, D. A., Kalamkarov, A., and Georgiades, T., "Micromechanical Analysis of Piezo-Magneto-Thermo-Elastic T-Ribbed and II-Ribbed Plates," *Mechanics of Advanced Materials and Structures*, , No. just-accepted, 2017.

[36] Kollár, L. P., and Springer, G. S., *Mechanics of Composite Structures*, Cambridge University Press, 2003. doi:10.1017/CBO9780511547140.